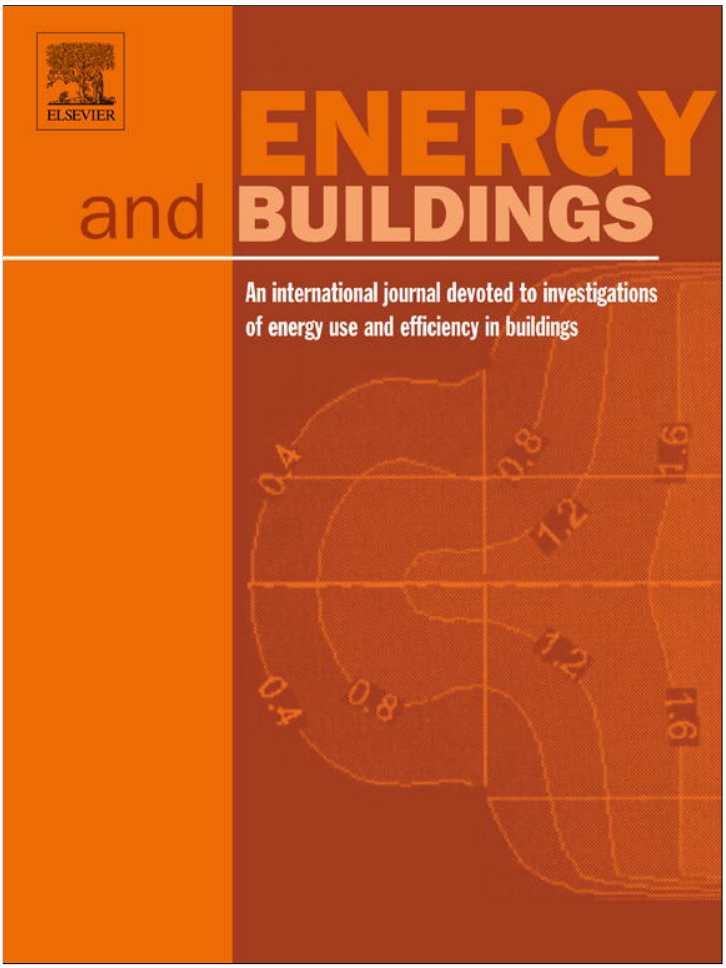

Energy and Buildings 62 (2013) 190–195

Contents lists available at SciVerse ScienceDirect

Energy and Buildings

journal homepage: www.elsevier.com/locate/enbuild

Preparation and evaluation of thermal enhanced silica fume by incorporating organic PCM, for application to concrete

Su-Gwang Jeong, Jisoo Jeon, Junghoon Cha, Junhyun Kim, Sumin Kim*

Building Environment & Materials Lab, School of Architecture, Soongsil University, Seoul, Republic of Korea

ARTICLE INFO

Article history:
Received 9 August 2012
Received in revised form 7 December 2012
Accepted 20 February 2013

Keywords:
PCM
Silica fume
Thermal properties
Cement
Heat storage

ABSTRACT

Silica fume has been used as a replacement for cement, due to its high early compressive strength, high tensile and flexural strength, high bond strength, and enhanced durability of concrete. This study examined enhanced thermal performances of silica fume by incorporating organic PCMs, for applying to concrete. Three kinds of organic PCMs were incorporated into the silica fume. The silica fume/PCM composites were prepared by the vacuum impregnation method. Because silica fume has a high porous structure compared to cement, it is useful to incorporate the PCM, to enhance its thermal storage performance. The characteristics of the composites were determined by using SEM, DSC, FTIR and TGA. SEM morphology showed the micro-structure of silica fume/PCM. Also, thermal properties were examined by DSC and TGA analyses; and the chemical bonding of the composite was determined by FTIR analysis.

1. Introduction

Recently, the use of thermal energy storage with phase change material (PCM) is considered to be one of the most important advanced technologies, and a lot of attention has been paid to utilization of the essential techniques for thermal applications, ranging from heating to cooling in buildings. Using thermal energy storage system in a building can smooth temperature fluctuation, and such storage can be implemented by sensible heat, or latent heat [1]. Latent heat storage enables the passive control of temperature in buildings. The latent heat storage method provides a much higher heat storage density, with a smaller temperature difference between storage and release of heat [2]. PCMs are divided into three kinds: organic PCM, inorganic PCM and eutectic PCM. These are used as storage media in latent thermal energy storage, and can be classified into two major categories: organic and inorganic compounds. Inorganic PCMs include salt hydrates, salts, metals and alloys; whereas organic PCMs are comprised of hexadecane, octadecane, paraffin, fatty acids/esters, etc. Also, eutectic PCMs mean mixtures of PCMs, which are made by composition of organic–organic, organic–inorganic and inorganic–inorganic PCMs. Because organic PCMs have various advantages, most researchers have studied organic PCM in their research. Among the investigated PCMs, organic PCMs have been widely used in thermal energy storage applications, due to their large latent heat, and proper thermal characteristics, such as little or no super cooling, low vapor pressure, good thermal and chemical stability, and self-nucleating behavior [3–9]. However, the application of PCMs to various fields is difficult, due to their phase instability in the liquid state. Therefore, PCMs need shape stabilization. To solve these problems, some investigators have studied the possibility of a container that can prevent the leaking of liquid PCMs, by using shape-stabilized PCM (SSPCM), microencapsulated PCM (MPCM), and incorporated PCM techniques [10–15]. Actually, PCM should be incorporated into building construction materials, such as gypsum wallboard, plaster, concrete, clay minerals, and other wall covering material [16,17]. Therefore this paper has used silica fume as a container of PCM. Silica fume has been used as a replacement for cement, due to its high early compressive strength, high tensile and flexural strength, high bond strength, and enhanced durability of concrete. Silica fume is a by-product from electric furnaces, used in the manufacture of silicon metal or silicon alloys. These advantages of silica fume derive from the high specific surface, and the pozzolanic activity of silica fume particles [18–23]. Considering all these features mentioned above, silica fume is one of the feasible candidates for an economical and light-weight building material, to incorporate PCM for thermal energy storage in buildings. Therefore in this study, enhanced thermal performances of silica fume were examined for applying to concrete, by incorporating organic PCMs. In order to increase the impregnation amount of PCM in porous silica fume, the vacuum impregnation technology is applied during the fabrication process [24]. The vacuum impregnation method guarantees heat storage of PCM after the incorporation process. Therefore, this paper addresses the enhancing of thermal properties of the silica fume. Also, we evaluated the applicability of PCM/silica fume composites for applying to concrete using silica fume, which replaces

* Corresponding author. Tel.: +82 2 820 0665; fax: +82 2 816 3354.
E-mail address: skim@ssu.ac.kr (S. Kim).

0378-7788/$ – see front matter.
http://dx.doi.org/10.1016/j.enbuild.2013.02.053

Table 1
Physical properties of cement and silica fume.

Physical properties of cement and silica fume	Cement	Silica fume
Particle mean diameter (μm)	7.4	6.3
BET specific surface area (m^2/g)	9.6	220
True density (g/cm^3)	2.29	2.93
Porosity	0.45	0.84

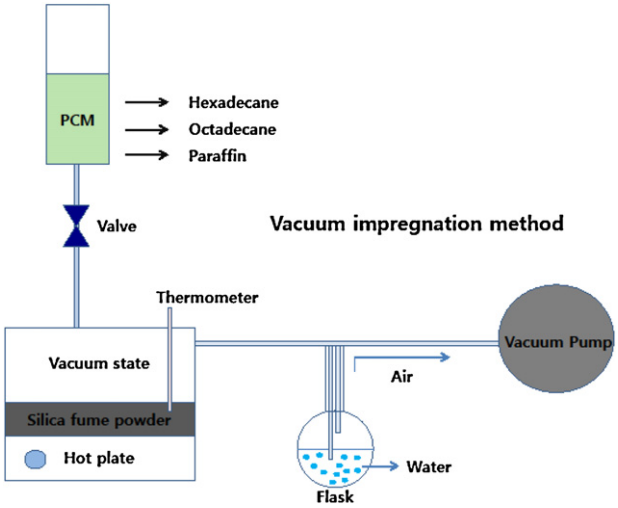

Fig. 1. A schematic of the vacuum impregnation method.

the cement. This paper analyzed the micro-structure, chemical bonding, heat capacity and thermal durability of PCM/silica fume composites, from the results of SEM, FTIR, DSC and TGA analysis.

2. Experimental

2.1. Materials

In this experiment, we used three types of PCMs to incorporate the silica fume. Hexadecane, octadecane and paraffin were used for the experiment as heat storage materials. These PCMs have different phase change ranges, of 20.84 °C, 30.4 °C and 57.09 °C, respectively, and latent heat capacities of 254.7 J/g, 247.6 J/g and 144.6 J/g, respectively. The PCMs were obtained from the Celsius Korea company in South Korea. The silica fume was supplied from Taiwang, a leading international trading company in South Korea. This silica is a powder type, and has sold well in the concrete market as a replacement material for cement. The typical bulk density of silica fume is 200–350 kg/m^3, and the silica fume contains over 85% SiO_2. Before the experiment, the silica fume was placed in a container, and the sample was dried at 80 °C for 5 h. Silica fume has a good structure for incorporating PCM into itself, compared to cement. Table 1 shows the physical properties of cement and silica fume [25]. Also, Table 2 shows the major components of silica fume.

2.2. Preparation

The PCM/silica fume composite was prepared using vacuum impregnation. A schematic of the vacuum impregnation system is shown in Fig. 1. The dried silica fume sample was put in a flask, which was connected to a round bottom flask to evacuate air from the porous structure of silica fume. Then, the valve between the flask and the container with liquid PCM was opened, to let PCM into the flask to impregnate the silica fume. The vacuum process was continued for 90 min, and then air was allowed to enter the flask again, to force the liquid PCM to penetrate into the porous structure of the silica fume. Then we carried out a filtering process, to remove the extra PCM in the PCM/silica fume composite. The colloidal state was filtered by 1 μm filter paper, until a granular sample appeared, which was dried in a vacuum drier at 80 °C for 24 h, 48 h and 72 h, for hexadecane, octadecane, and paraffin, respectively.

2.3. Characterization methods

We carried out scanning electron microscopy (SEM), Fourier transform infrared spectroscopy (FTIR: 300EJasco), differential scanning calorimetry (DSC:Q1000) and thermo gravimetric analysis (TGA: TA Instruments, TGA Q5000). To confirm the morphology and micro-structure of composites, we performed the SEM analysis at room temperature. A SEM with an accelerating voltage of 12 kV and working distance of 12 mm was used to collect the SEM images. The samples were coated with a gold coating of a few nano meters in thickness [26]. FTIR was also utilized, to monitor the changes of chemical groups upon curing. Clear potassium bromide discs were molded from powder, and used as backgrounds. The samples were analyzed over the range of 525–4000 cm^{-1}, with a spectrum resolution of 4 cm^{-1}. All spectra were averaged over 32 scans. This analysis of the composites was performed by point-to-point contact with a pressure device [27]. Thermal properties of pure PCMs and composite PCMs, such as the melting temperature and latent heat capacity, were measured using a DSC apparatus. The melting temperature was measured by drawing a line at the point of maximum slope of the leading edge of the peak, and extrapolating to the baseline [10]. The latent heat of the samples was determined by numerical integration of the area under the peaks that represent the solid–solid and solid–liquid phase transitions. Using a TGA, thermo gravimetric analysis measurements of the samples were carried out, on approximately 2–4 mg samples over the temperature range 25–600 °C, at a heating rate of 10 °C/min under a nitrogen flow of 20 ml/min. TGA was measured, with the composites placed in a high quality nitrogen (99.5% nitrogen, 0.5% oxygen content) atmosphere, to prevent unwanted oxidation [28].

3. Results and discussion

3.1. Morphology and microstructures of silica fume with impregnated PCM

Fig. 2 shows the morphology of the PCM composites that were included in the container. When we see the PCM composites with the naked eye, they seem to be well dispersed into the silica fume's structure. In this study, we confirmed that the minimum mixture ratio of PCM was secured in the structure of silica fume. Each PCM composite is shown, as these samples have different morphologies. In the case of hexadecane composite, this was prepared as a powder type after the manufacturing process, compared to the other PCM composites. The octadecane composite and paraffin composite were made with a granule type. However, although they had different types of shape, leakage phenomenon due to the liquid PCM did

Table 2
Components and ignition loss of silica fume.

SiO_2 (%)	Al_2O_3 (%)	FE_2O_3 (%)	CaO (%)	MgO (%)	Na_2O (%)	K_2O (%)	SO_3 (%)	Ig. loss (ignition loss)
85–95	≤1.5	≤3.0	≤0.7	≤2.0	–	–	≤0.2	≤3.0

Fig. 2. Sample images of PCM/silica fume composites: (a) hexadecane/silica fume composite, (b) octadecane/silica fume composite, and (c) paraffin/silica fume composite.

not occur in the container under the high temperature condition. This result showed that the PCM was well incorporated into the structure of silica fume. Also, no leakage properties of PCM composite were revealed by SEM analysis, as shown in Fig. 3. Fig. 3(a) shows the micro-structure of natural silica fume. As seen in Table 1, silica fume is more porous than cement; and we found from the BET (Brunauer–Emmett–Teller equation) analysis that the specific surface area is larger than that of cement. As mentioned above, silica fume has a good structure for incorporating PCM, compared to cement. From Fig. 3(a), silica fume has a porous structure compared to Fig. 3(b), which is the micro-structure of cement. As can be seen in Fig. 3(c)–(e), we found that many porous parts of the silica fume have disappeared. This means that each PCM was incorporated well into the structure of the silica fume. In the case of paraffin, the micro-structure image is dissimilar to the other PCM/silica fume composites. This shows the unique characteristics of paraffin. As a result, from the micro-structure analysis, silica fume could contain the PCM, and PCM maintained its thermal properties after the incorporation process.

3.2. Chemical combination analysis

The FTIR absorption spectra of the PCM/Silica fume composites are shown in Fig. 4. This experiment was carried out to check whether or not there was the characteristic of chemical bonding. As can be seen in Table 2, the silica fume is composed of more than 85% silica. So, the silica peak showed in the FTIR graph. The most intense band at 1085 cm^{-1} is due to asymmetric stretching of the Si—O—Si bonding. This band usually appears between 1200 and 1000 cm^{-1}. Not only is this band very intense, but it has an asymmetric shape, which can be used as a diagnostic marker for the presence of silica

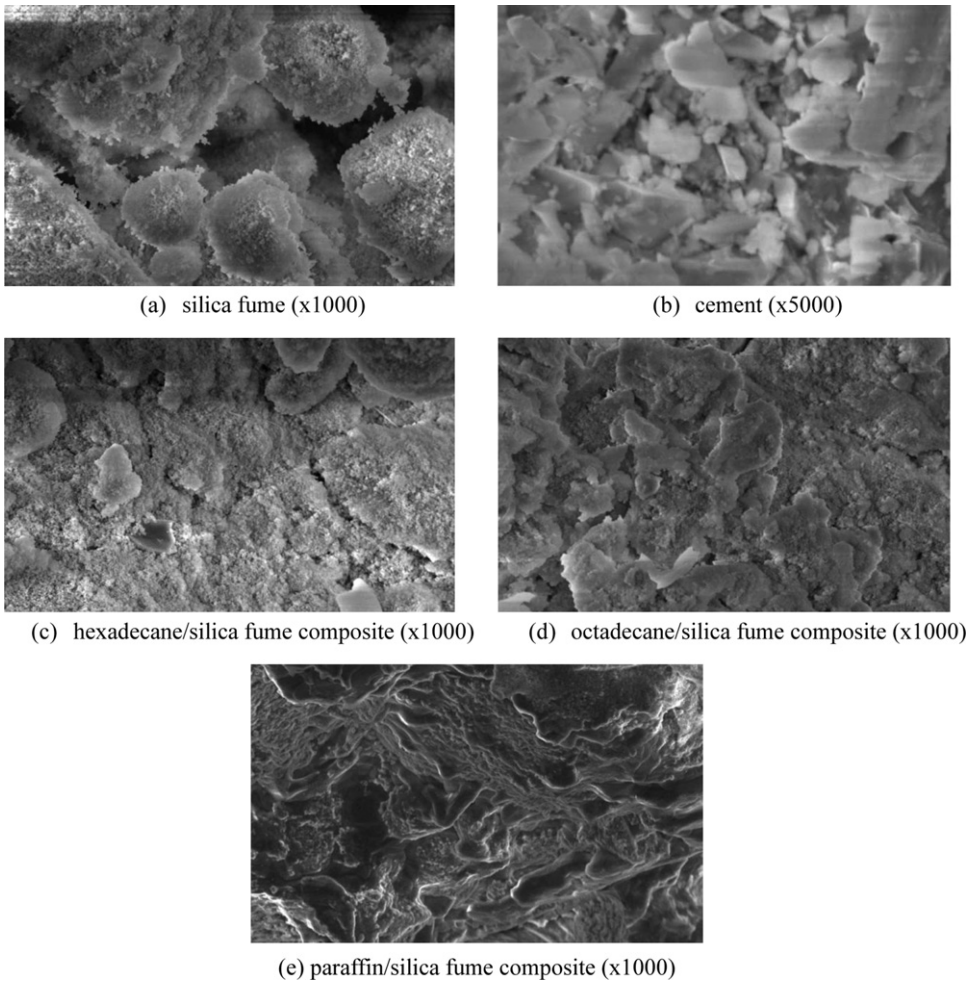

Fig. 3. SEM analysis of PCM/silica fume composites: (a) silica fume, (b) cement, (c) hexadecane/silica fume composite, (d) octadecane/silica fume composite, and (e) paraffin/silica fume composite.

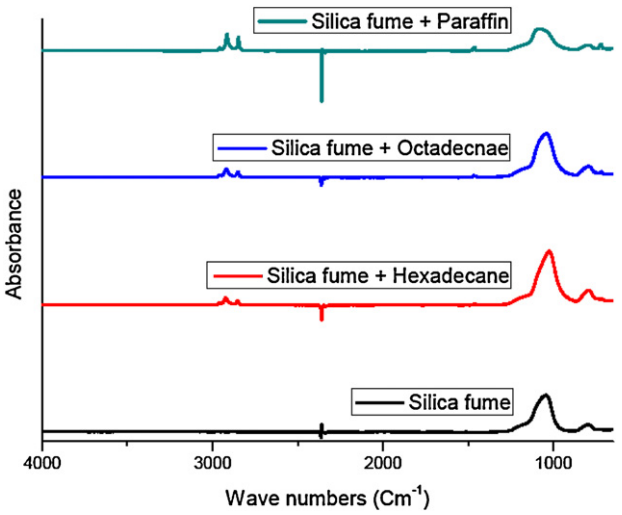

Fig. 4. FTIR analysis of PCM/silica fume composites.

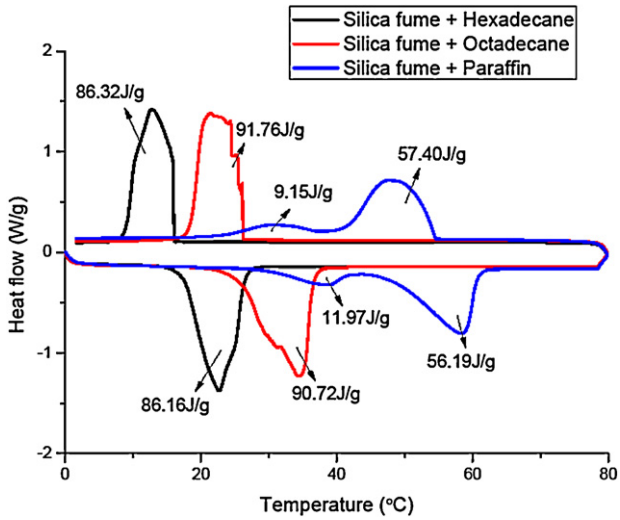

Fig. 5. DSC analysis of PCM/silica fume composites.

in a sample. These stretching vibration bands have appeared after the compositing process with PCMs. This means that the chemical properties of silica fume were not changed. Also, the hexadecane, octadecane and paraffin have the same FTIR peaks, because these PCMs have a similar molecular structure, which is $C_nH_{(2n+2)}$. So the peaks of these PCMs show the stretching vibration of functional groups of $-CH_2$ and $-CH_3$. These FTIR absorption spectra have peaks of 2954, 2955 and 2961 cm^{-1}, which were caused by $C-H_3$ asymmetric stretch, and of 2870 and 2876 cm^{-1}, which were caused by $C-H_3$ symmetric stretch. Also, the 2920 and 2860 cm^{-1} peaks were caused by $C-H_2$ groups. As a result, these peaks of PCMs have not disappeared from the FTIR graphs. Whole peaks of the silica fume and PCM have not changed, and have not disappeared. Therefore, this means that these composites are composed of the PCM and silica fume by mechanical bonding. So the thermal properties of PCM were maintained in the structure of the silica fume; and after applying mortar or concrete, its latent heat storage performance would be revealed (Table 3).

3.3. Latent heat storage analysis

The DSC curves of PCM/silica fume composites during heating and subsequent cooling are presented in Fig. 5. As can be clearly seen, the hexadecane/silica fume, octadecane/silica fume and paraffin/silica fume melt at 22.32, 33.61 and 58.39 °C, respectively; also they freeze at 12.85, 22.48 and 49.04 °C, respectively. Three types of phase change temperature range are shown. This graph shows the melting peaks of composite PCMs have a high temperature range, because the PCMs were influenced by supercooling. The latent heat peak and peak temperature, regarding the melting and freezing of the composite PCMs, are also given in Table 4. The latent heat capacities are obtained by numerical integration of the total area under the peaks of the solid–liquid transition curves of the PCMs in the composite. The latent heat capacities of each PCM are indicated at 86.16, 90.72 and 56.19 J/g during the melting process; also they release 86.32, 91.76 and 57.40 J/g of latent heat during the freezing process. As shown in the paraffin peak line, it can be seen that paraffin has two phase change peaks. The sharp or main peak near 58 °C represents the solid–liquid phase change of paraffin, and the minor peak on the left side of the main peak corresponds to the solid–solid phase transition of paraffin. The first peak of the paraffin/silica fume indicates 11.97 and 9.15 J/g, during the melting and freezing processes. However, its latent heat capacity is small. Also, it is not difficult to find that the latent heat peaks of PCM still exist in the PCM/silica fume composites. The thermal characteristics of the PCM/silica fume composites, such as the melting and freezing temperatures, approach those of pure PCMs. This is because the PCMs are composed of silica fume, and there are no chemical reactions among PCM and silica fume during the impregnating process. Also, the incorporation rate of each PCM is 33.8, 36.6 and 38.8% of value for the pure PCMs. Although the latent heat capacity of the PCM/silica fume shows a slight decrease, compared to the pure PCMs, it is still enough to apply to a building material, such as concrete. Therefore, considering applications in building materials, during the phase change from solid to liquid the PCM/silica fume can still act to prevent the leakage of paraffin occurring. As a result, we confirmed that the latent heat properties of PCM remained in the pores of the silica fume, and we expect that the PCM/silica fume composites can be used as thermal energy storage material, to apply to building material.

Table 3
FTIR spectra of the PCM/silica fume composites.

Vibration	Wave number range (cm^{-1})
Si—O—Si asymmetric stretch	1200–1000
Silanol Si—O stretch	944
Si—O—Si symmetric stretch	802
$C-H_3$ asymmetric stretch	2954, 2955, 2961
$C-H_3$ symmetric stretch	2870, 2876
$C-H_2$ asymmetric stretch	2920
$C-H_2$ symmetric stretch	2860

3.4. Thermal durability of PCM/silica fume composites

TGA is frequently used to analyze the thermal-durable property of PCMs. This property is important, because processes to manufacture various PCM products are subject to high temperature. The thermal durability property is one of the most important parameters for a composite PCM used in thermal energy storage applications, because it should be durable over its working temperatures. The thermal durability limits of the prepared composite PCMs were investigated by TGA analysis. TGA curves of PCM/silica fume composites are shown in Fig. 6. As shown in the graph, the weight loss processes of the PCM/silica fume composites were carried out in one step. In the case of the hexadecane/silica fume composite, the initial degradation step started at 150 °C, and finished at 200 °C. This degradation means that oxidation of hexadecane, and also octadecane/silica composite, showed similar

Table 4
Heat storage properties of PCM/silica fume composites.

PCM samples	Melting point (°C)	Freezing point (°C)	Latent heat (J/g)				Incorporated rate (%)
			Solid–solid melting	Solid–solid freezing	Solid–liquid melting	Liquid–solid freezing	
Hexadecane/silica fume	22.32	12.85	–	–	86.16	86.32	33.8
Octadecane/silica fume	33.61	22.48	–	–	90.72	91.76	36.6
Paraffin/silica fume	58.39	49.04	11.97	9.15	56.19	57.40	38.8

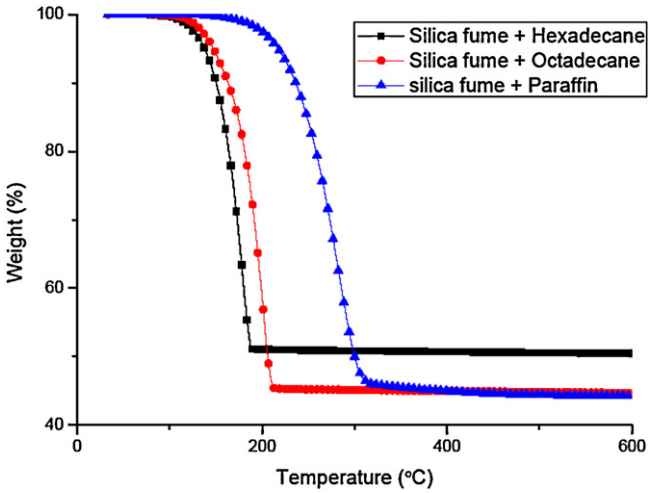

Fig. 6. Thermal gravimetric analysis of PCM/silica fume composites.

behavior. However, the thermal degradation curve of paraffin/silica fume composite started at 200 °C, which is higher than the other composite PMCs. This means paraffin has a high thermal durability property. For the hexadecane/silica fume, 50% of weight loss occurred between 150 and 200 °C. As also seen from the octadecane/silica fume and paraffin/silica fume, composites lost 55% of their weight in the range of 150–200 °C and 200–300 °C, respectively. Generally, PCM/silica fume composites show 50–55% degradation of weight. This means that the weight degradation of PCM/silica fume is attributed to the oxidation of PCM. Also, we determined that the silica fume remained after the oxidizing process. This shows that the PCM incorporated into the structure of silica fume, and the high thermally durable properties of silica fume, led to an enhancement of the thermal durability of the PCM/silica fume composite. As a result, we determined that silica fume supplied not only the porous space to incorporate the PCM, but also its thermal retardant properties.

4. Conclusion

Recently, many studies have been carried out on the reduction of energy consumption. Therefore, we prepared PCM/silica fume composites for the reduction of energy, by improving thermal efficiency through latent heat storage. We manufactured these samples to apply to a building material, such as concrete. PCM/silica fume composites designed to produce high thermal performance were prepared through vacuum impregnation. Impregnation of PCM is one way to prevent leakage of liquid state PCM, and vacuum treatment is effective in conserving the thermal properties of pure PCM. We carried out experiments to confirm the characteristics of the PCM/silica fume composites, using SEM, FTIR, DSC and TGA analyses. SEM analysis showed that each PCM was completely incorporated into the pores of the silica fume. The peaks of pure PCM and silica fume are still shown in the PCM/silica fume composites peaks from the TGA analysis, because PCM/silica fume composites are composed of mechanical bonding between the pure PCMs and the silica fume. From the latent heat storage analysis, we confirmed that the PCM/silica fume composites have high latent heat storages, since each PCM was well incorporated into the structure of silica. Also, we found that the high thermally durable properties of silica fume led to an enhancement of the thermal durability of the PCM/silica fume composites. Consequently, we expect the PCM/silica fume composites to be useful for applying to building materials, such as concrete, due to the shape stability characteristics and high thermal performance of PCM/silica fume composite. In future research, this experiment needs to be expanded, in order to obtain high heat storage properties and thermal durability.

Acknowledgements

This work was supported by a National Research Foundation of Korea (NRF) grant, funded by the Korea government (MEST) (No. 2012-0005188). This works is financially supported by the Advanced Track of Green Production Processing for Reducing Greenhouse Gas Emission of the KETEP grant funded by Ministry of Knowledge Economy (No. 20114010203140).

References

[1] L.F. Cabeza, A. Castell, C. Barreneche, A. de Gracia, A.I. Fernández, Materials used as PCM in thermal energy storage in buildings: a review, Renewable and Sustainable Energy Reviews 15 (2011) 1675–1695.
[2] X. Zhang, P. Deng, R. Feng, J. Song, Novel gelatinous shape-stabilized phase change materials with high heat storage density, Solar Energy Materials and Solar Cells 95 (2011) 1213–1218.
[3] A. Abhat, Low temperature latent heat thermal energy storage: heat storage materials, Solar Energy 30 (1983) 313–332.
[4] B. Zalba, J.M. Marĩn, L.F. Cabeza, H. Mehling, Review on thermal energy storage with phase change: materials, heat transfer analysis and applications, Applied Thermal Engineering 23 (2003) 251–283.
[5] S.D. Sharma, K. Sagara, Latent heat storage materials and systems: a review, International Journal of Green Energy 2 (2005) 1–56.
[6] A. Sari, Form-stable paraffin/high density polyethylene composites as solid–liquid phase change material for thermal energy storage: preparation and thermal properties, Energy Conversion and Management 45 (2004) 2033–2042.
[7] Z. Zhang, X. Fang, Study on paraffin/expanded graphite composite phase change thermal energy storage material, Energy Conversion and Management 47 (2006) 303–310.
[8] Y. Zhang, J. Ding, X. Wang, R. Yang, K. Lin, Influence of additives on thermal conductivity of shape-stabilized phase change material, Solar Energy Materials and Solar Cells 90 (2006) 1692–1702.
[9] X. Liu, H. Liu, S. Wang, L. Zhang, H. Cheng, Preparation and thermal properties of form stable paraffin phase change material encapsulation, Energy Conversion and Management 47 (2006) 2515–2522.
[10] S. Jeong, J. Jeon, J. Seo, J. Lee, S. Kim, Performance evaluation of the microencapsulated PCM for wood-based flooring application, Energy Conversion and Management (2012), published online.
[11] X. Wang, J. Niu, A.H.C. van Paassen, Raising evaporative cooling potentials using combined cooled ceiling and MPCM slurry storage, Energy and Buildings 40 (2008) 1691–1698.
[12] X. Xu, Y. Zhang, K. Lin, H. Di, R. Yang, Modeling and simulation on the thermal performance of shape-stabilized phase change material floor used in passive solar buildings, Energy and Buildings 37 (2005) 1084–1091.
[13] B.M. Diaconu, Transient thermal response of a PCS heat storage system, Energy and Buildings 41 (2009) 212–219.
[14] P. Zhang, Y. Hu, L. Song, J. Ni, W. Xing, J. Wang, Effect of expanded graphite on properties of high-density polyethylene/paraffin composite with intumescent flame retardant as a shape-stabilized phase change material, Solar Energy Materials and Solar Cells 94 (2010) 360–365.

[15] Y. Wang, T.D. Xia, H. Zheng, H.X. Feng, Stearic acid/silica fume composite as form-stable phase change material for thermal energy storage, Energy and Buildings 43 (2011) 2365–2370.
[16] P. Schossig, H.-M. Henning, S. Gschwander, T. Haussmann, Micro-encapsulated phase-change materials integrated into construction materials, Solar Energy Materials and Solar Cells 89 (2005) 297–306.
[17] A. Karaipekli, A. Sari, Capric–myristic acid/expanded perlite composite as form-stable phase change material for latent heat thermal energy storage, Renewable Energy 33 (2008) 2599–2605.
[18] W. Wongkeo, A. Chaipanich, Compressive strength, microstructure and thermal analysis of autoclaved and air cured structural lightweight concrete made with coal bottom ash and silica fume, Materials Science and Engineering: A 527 (2010) 3676–3684.
[19] M. Barati, S. Sarder, A. McLean, R. Roy, Recovery of silicon from silica fume, Journal of Non-Crystalline Solids 357 (2011) 18–23.
[20] M.S. Amin, F.S. Hashem, Hydration characteristics of hydrothermal treated cement kiln dust–sludge–silica fume pastes, Construction and Building Materials 25 (2011) 1870–1876.
[21] M. Mazloom, A.A. Ramezanianpour, J.J. Brooks, Effect of silica fume on mechanical properties of high-strength concrete, Cement and Concrete Composites 26 (2004) 347–357.
[22] H. Song, S. Pack, S. Nam, J. Jang, V. Saraswathy, Estimation of the permeability of silica fume cement concrete, Construction and Building Materials 24 (2010) 315–321.
[23] G.I. Sezer, Compressive strength and sulfate resistance of limestone and/or silica fume mortars, Construction and Building Materials 26 (2012) 613–618.
[24] A. Sari, A. Karaipekli, Preparation, thermal properties and thermal reliability of palmitic acid/expanded graphite composite as form-stable PCM for thermal energy storage, Solar Energy Materials and Solar Cells 93 (2009) 571–576.
[25] R. Lin, S. Shih, C. Liu, Characteristics and reactivities of $Ca(OH)_2$/silica fume sorbents for low-temperature flue gas desulfurization, Chemical Engineering Science 58 (2003) 3659–3668.
[26] S. Kim, L.T. Drzal, High latent heat storage and high thermal conductive phase change materials using exfoliated graphite nanoplatelets, Solar Energy Materials and Solar Cells 93 (2009) 136–142.
[27] H. Kim, B. Lee, S. Choi, S. Kim, H. Kim, The effect of types of maleic anhydride-grafted polypropylene (MAPP) on the interfacial adhesion properties of bio-flour-filled polypropylene composites, Composites Part A: Applied Science and Manufacturing 38 (2007) 1473–1482.
[28] B. Lee, H. Kim, H. Yang, Polymerization of aniline on bacterial cellulose and characterization of bacterial cellulose/polyaniline nanocomposite films, Current Applied Physics 12 (2012) 75–80.